3GPP TSG RAN WG1 Meeting #87 R1-1612308
Reno, Nevada, USA, 14th – 18th November 2016

Agenda item: 7.1.5.1
Source: AccelerComm
Title: BLER performance of list decoding for enhanced turbo codes
Document for: Discussion

I. Introduction

This paper presents Block Error Ratio (BLER) performance results for the list decoding of the enhanced turbo code of [1]. The list decoding technique of [2] is employed, as implemented in the attached Matlab code. Here, a list Viterbi decoder [3] is employed to identify a list comprising the L most likely paths through the trellis of the upper component code. Following this L replicas of the iterative turbo decoding process are performed. During the first iteration of each replica, a different set of transitions are pruned from the trellis of the upper component code, in order to force a different starting point for the turbo decoding process. At the completion of the L turbo decoding processes, L different decoded bit sequences are typically obtained. Therefore, the complexity of list turbo decoding is equal to the L times the complexity of conventional turbo decoding, plus the complexity of a list Viterbi decoder.

The BLER results presented in this paper quantify the ratio of information blocks that do not exist within the list of L decoded candidates.

II. eMBB data channel

Figures 1 – 3 provide BLER results for block lengths of $K \in \{96, 400, 992\}$ bits, when using Quaternary Phase Shift Keying (QPSK) modulation for transmission over an Additive White Gaussian Noise (AWGN) channel. Likewise, Figure 4 provides BLER results for a block length of $K = 96$ bits, when using QPSK modulation for transmission over an uncorrelated narrowband Rayleigh fading channel. Figure 5 provides BLER results for a block length of $K = 96$ bits, when using 64-ary Quadrature Amplitude Modulation (64QAM) modulation for transmission over an AWGN channel. Figure 6 provides BLER results for a block length of $K = 96$ bits, when using 64QAM modulation for transmission over an uncorrelated narrowband Rayleigh fading channel.

In all plots, $I = 8$ iterations of scaled-Max-Log-MAP decoding is assumed for coding rates of $R \in \{1/5, 1/3, 2/5, 1/2, 2/3, 8/9\}$ and list sizes of $L \in \{32, 16, 8, 4, 2, 1\}$.

III. eMBB control, uRLLC and mMTC channels

Figures 7 – 9 provide BLER results for block lengths of $K \in \{32, 80, 208\}$ bits, when using QPSK modulation for transmission over an AWGN channel. Likewise, Figures 10 – 12 provide BLER results for block lengths of $K \in \{32, 80, 208\}$ bits, when using QPSK modulation for transmission over an uncorrelated narrowband Rayleigh fading channel. Figures 13 and 14 provide BLER results for block lengths of $K \in \{32, 80\}$ bits, when using 64QAM modulation for transmission over an AWGN channel. Likewise, Figures 15 and 16 provide BLER results for block lengths of $K \in \{32, 80\}$ bits, when using 64QAM modulation for transmission over an uncorrelated narrowband Rayleigh fading channel.

In all plots, $I = 8$ iterations of scaled-Max-Log-MAP decoding is assumed for coding rates of $R \in \{1/12, 1/6, 1/3, 1/2, 2/3\}$ and list sizes of $L \in \{32, 16, 8, 4, 2, 1\}$.

IV. CONCLUSIONS

This paper has presented BLER performance results for the list decoding of the enhanced turbo code of [1].

Observation 1: List decoding of turbo codes provides greater coding gains when employing (a) higher list sizes L, (b) higher coding rates R, (c) shorter information block lengths K and/or (d) fading channels.

Observation 2: Relative to conventional turbo decoding, list decoding can provide coding gains of around 2 dB, when employing $L = 32$, $R = 2/3$, $K = 32$ and an uncorrelated Rayleigh fading channel.

REFERENCES

[1] Orange and IMT, "R1-1612938 Enhanced Turbo Codes for NR: Performance Evaluation for eMBB and URLLC," in *3GPP TSG RAN WG1 #87*, Nov. 2016.

[2] A. Akmalkhodzhaev and A. Kozlov, "New iterative turbo code list decoder," in *Proc. Int. Symp. Problems of Redundancy in Information and Control Systems*, June 2014, pp. 15–18.

[3] N. Seshadri and C. E. W. Sundberg, "List Viterbi decoding algorithms with applications," *IEEE Trans. Commun.*, vol. 42, no. 234, pp. 313–323, Feb 1994.

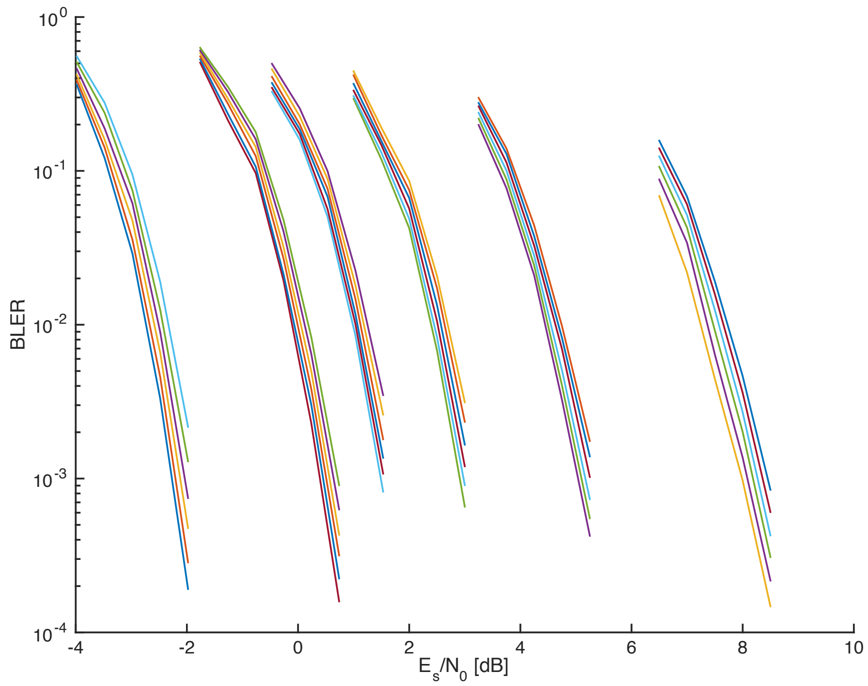

Fig. 1. $K = 96$. $R \in \{1/5, 1/3, 2/5, 1/2, 2/3, 8/9\}$ from left to right. $L \in \{32, 16, 8, 4, 2, 1\}$ from left to right. QPSK modulation. AWGN channel. $I = 8$ iterations of scaled-Max-Log-MAP decoding.

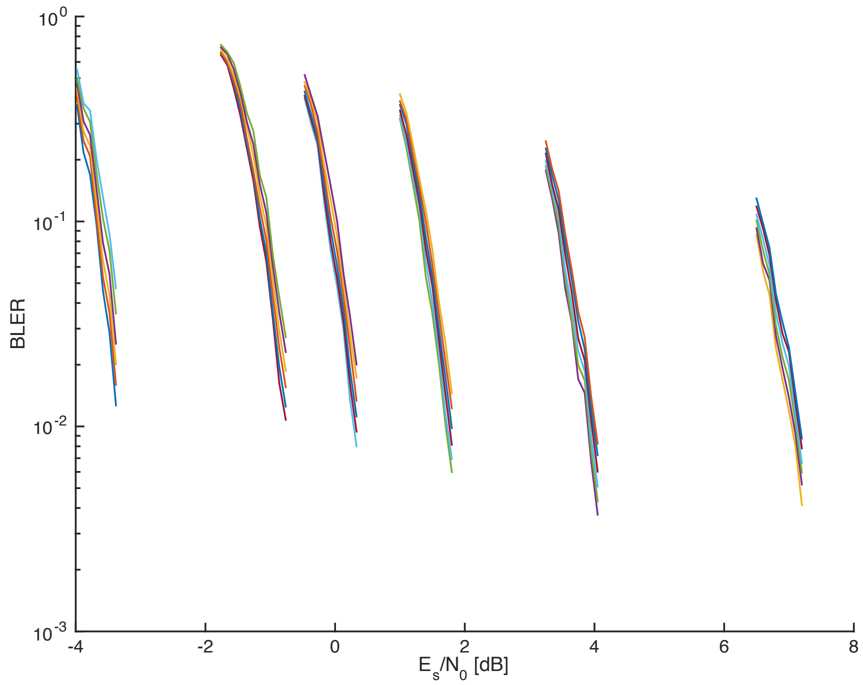

Fig. 2. $K = 400$. $R \in \{1/5, 1/3, 2/5, 1/2, 2/3, 8/9\}$ from left to right. $L \in \{32, 16, 8, 4, 2, 1\}$ from left to right. QPSK modulation. AWGN channel. $I = 8$ iterations of scaled-Max-Log-MAP decoding.

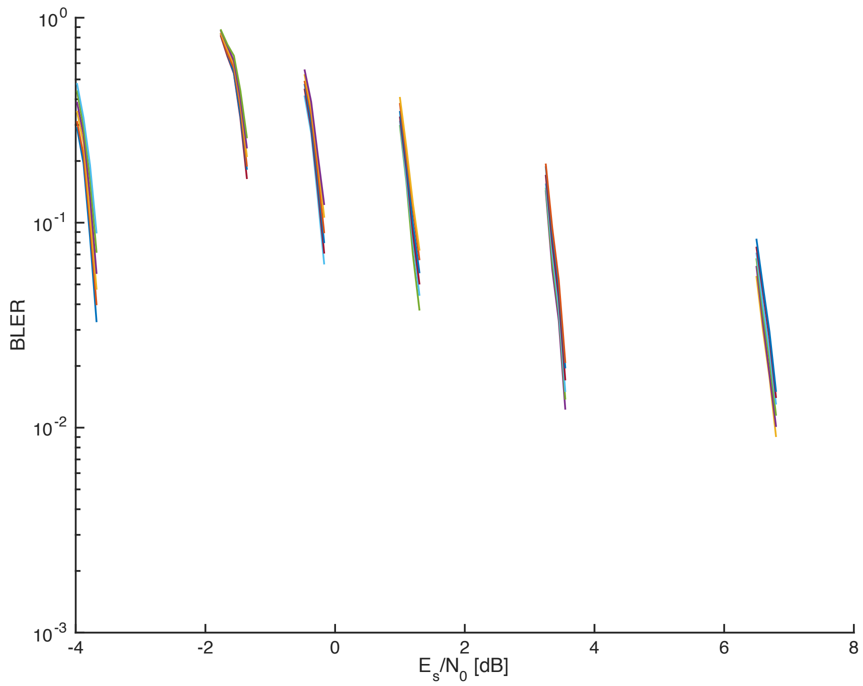

Fig. 3. $K = 992$. $R \in \{1/5, 1/3, 2/5, 1/2, 2/3, 8/9\}$ from left to right. $L \in \{32, 16, 8, 4, 2, 1\}$ from left to right. QPSK modulation. AWGN channel. $I = 8$ iterations of scaled-Max-Log-MAP decoding.

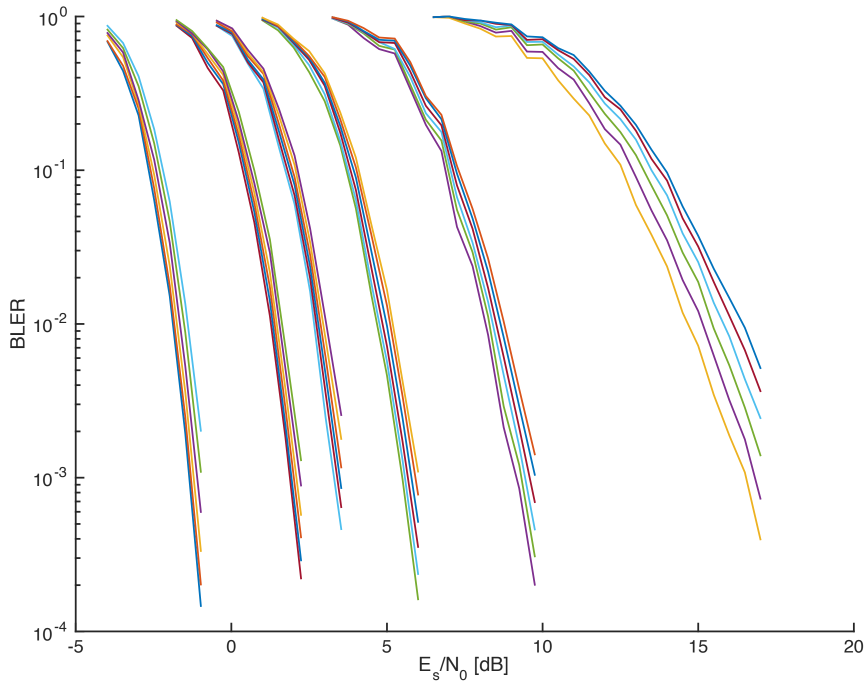

Fig. 4. $K = 96$. $R \in \{1/5, 1/3, 2/5, 1/2, 2/3, 8/9\}$ from left to right. $L \in \{32, 16, 8, 4, 2, 1\}$ from left to right. QPSK modulation. Uncorrelated narrowband Rayleigh fading channel. $I = 8$ iterations of scaled-Max-Log-MAP decoding.

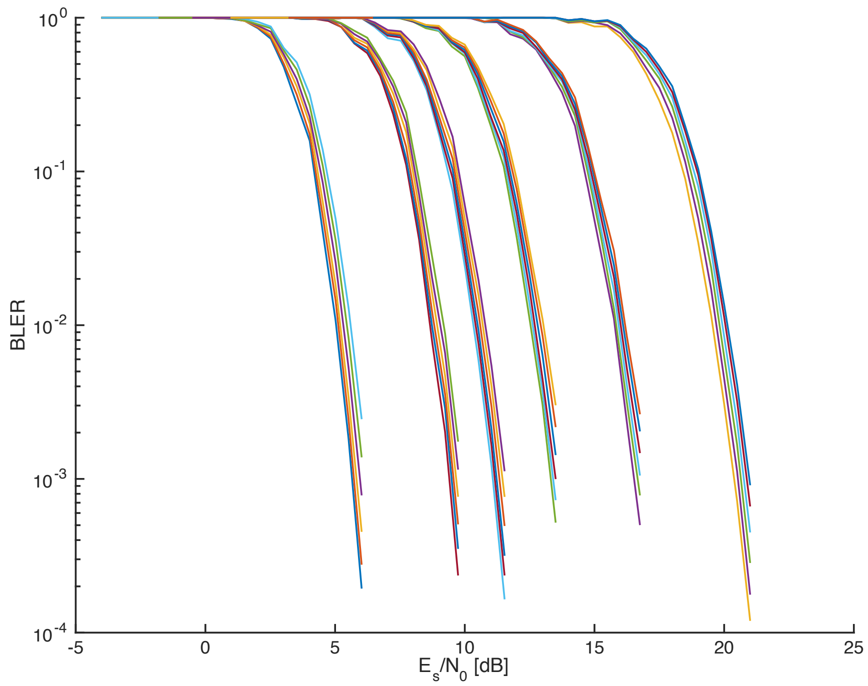

Fig. 5. $K = 96$. $R \in \{1/5, 1/3, 2/5, 1/2, 2/3, 8/9\}$ from left to right. $L \in \{32, 16, 8, 4, 2, 1\}$ from left to right. 64QAM modulation. AWGN channel. $I = 8$ iterations of scaled-Max-Log-MAP decoding.

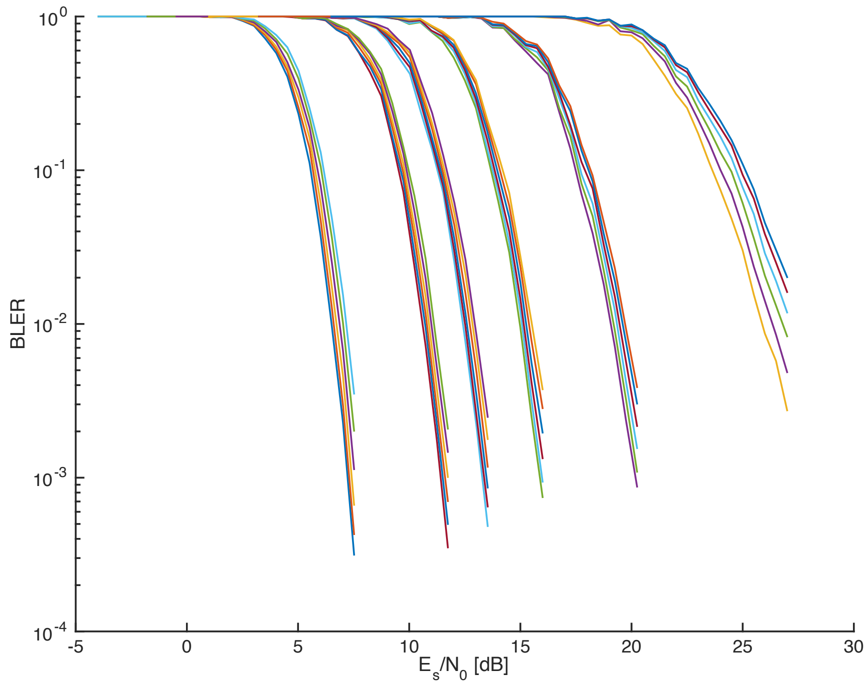

Fig. 6. $K = 96$. $R \in \{1/5, 1/3, 2/5, 1/2, 2/3, 8/9\}$ from left to right. $L \in \{32, 16, 8, 4, 2, 1\}$ from left to right. 64QAM modulation. Uncorrelated narrowband Rayleigh fading channel. $I = 8$ iterations of scaled-Max-Log-MAP decoding.

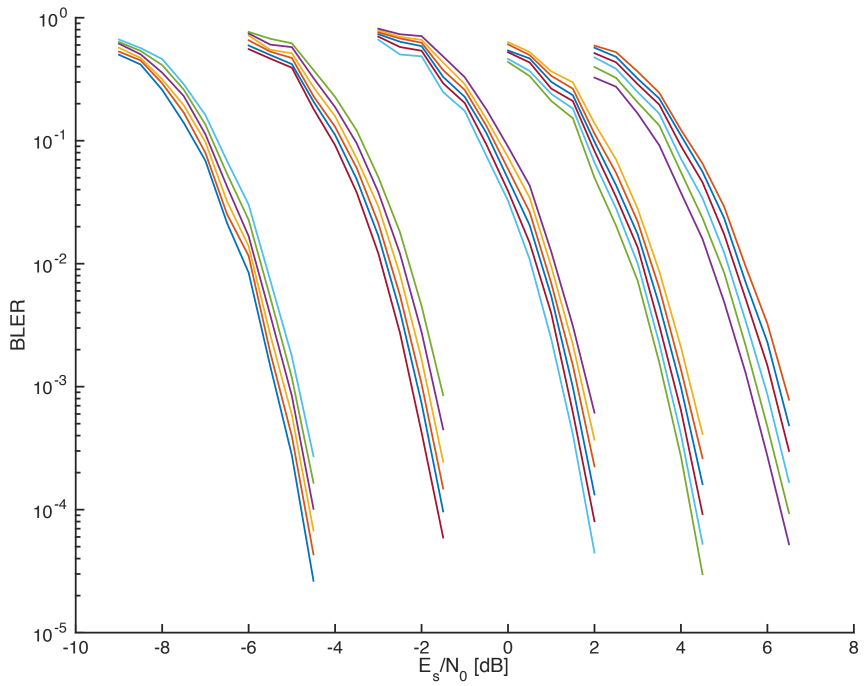

Fig. 7. $K = 32$. $R \in \{1/12, 1/6, 1/3, 1/2, 2/3\}$ from left to right. $L \in \{32, 16, 8, 4, 2, 1\}$ from left to right. QPSK modulation. AWGN channel. $I = 8$ iterations of scaled-Max-Log-MAP decoding.

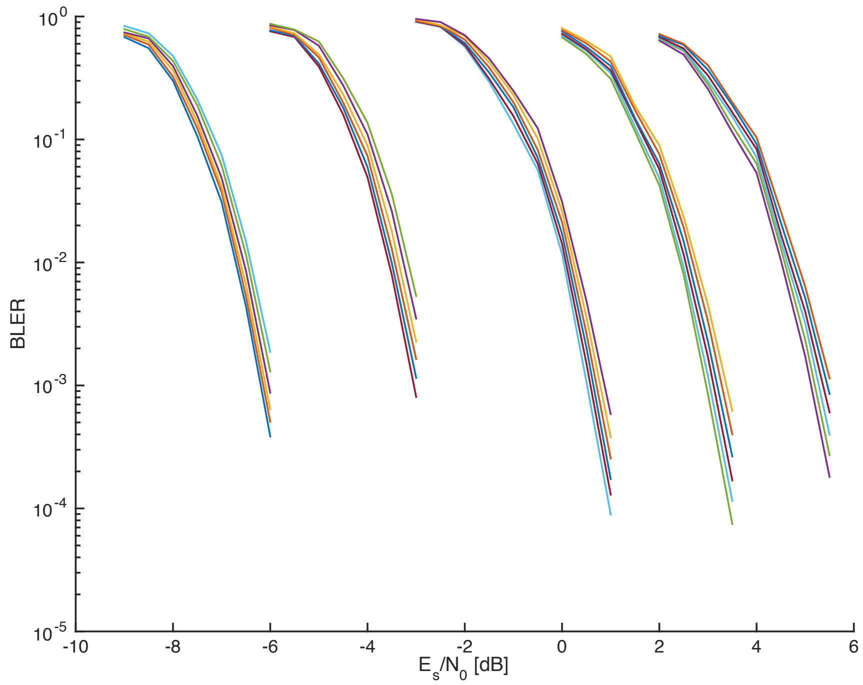

Fig. 8. $K = 80$. $R \in \{1/12, 1/6, 1/3, 1/2, 2/3\}$ from left to right. $L \in \{32, 16, 8, 4, 2, 1\}$ from left to right. QPSK modulation. AWGN channel. $I = 8$ iterations of scaled-Max-Log-MAP decoding.

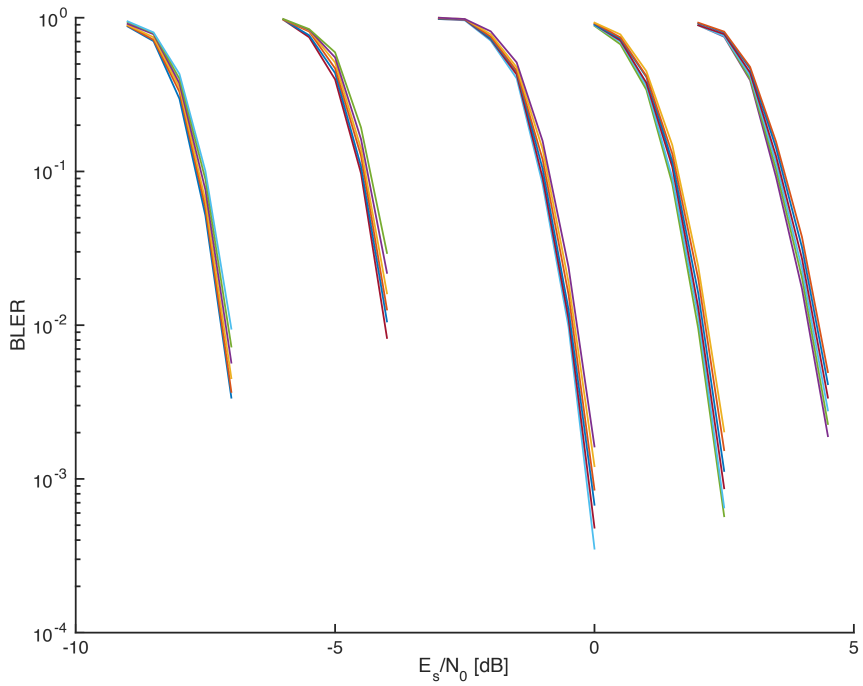

Fig. 9. $K = 208$. $R \in \{1/12, 1/6, 1/3, 1/2, 2/3\}$ from left to right. $L \in \{32, 16, 8, 4, 2, 1\}$ from left to right. QPSK modulation. AWGN channel. $I = 8$ iterations of scaled-Max-Log-MAP decoding.

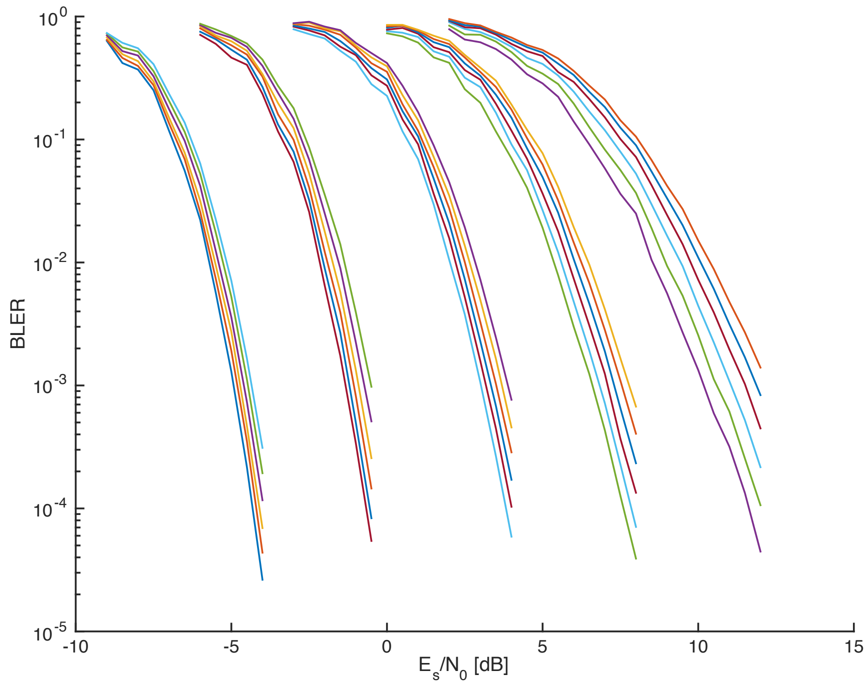

Fig. 10. $K = 32$. $R \in \{1/12, 1/6, 1/3, 1/2, 2/3\}$ from left to right. $L \in \{32, 16, 8, 4, 2, 1\}$ from left to right. QPSK modulation. Uncorrelated narrowband Rayleigh fading channel. $I = 8$ iterations of scaled-Max-Log-MAP decoding.

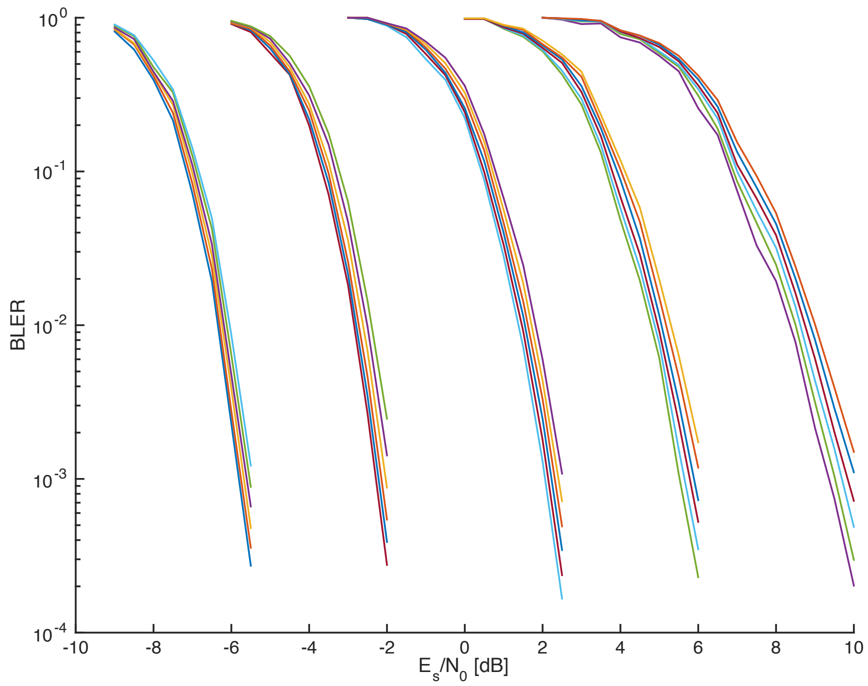

Fig. 11. $K = 80$. $R \in \{1/12, 1/6, 1/3, 1/2, 2/3\}$ from left to right. $L \in \{32, 16, 8, 4, 2, 1\}$ from left to right. QPSK modulation. Uncorrelated narrowband Rayleigh fading channel. $I = 8$ iterations of scaled-Max-Log-MAP decoding.

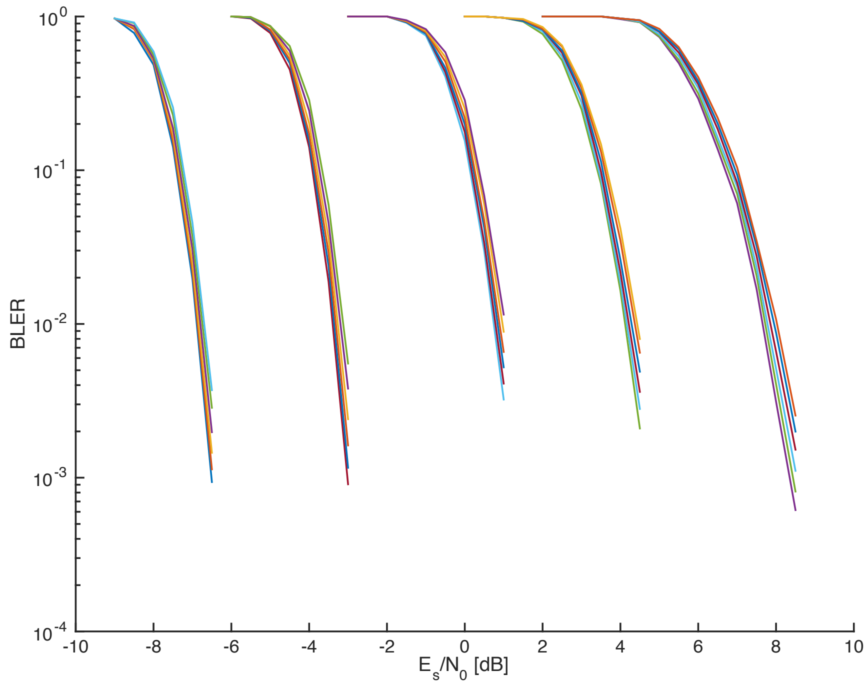

Fig. 12. $K = 208$. $R \in \{1/12, 1/6, 1/3, 1/2, 2/3\}$ from left to right. $L \in \{32, 16, 8, 4, 2, 1\}$ from left to right. QPSK modulation. Uncorrelated narrowband Rayleigh fading channel. $I = 8$ iterations of scaled-Max-Log-MAP decoding.

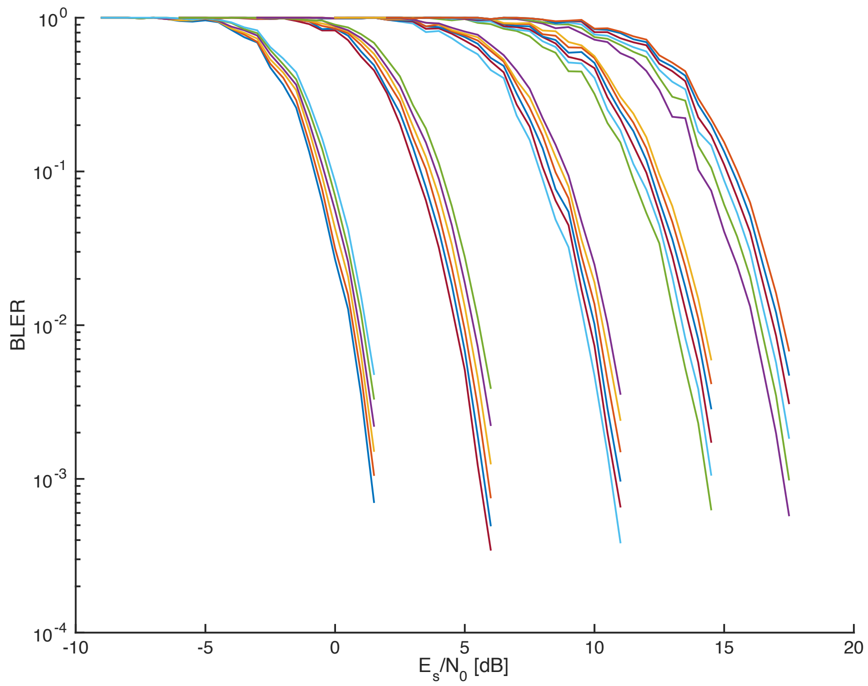

Fig. 13. $K = 32$. $R \in \{1/12, 1/6, 1/3, 1/2, 2/3\}$ from left to right. $L \in \{32, 16, 8, 4, 2, 1\}$ from left to right. 64QAM modulation. AWGN channel. $I = 8$ iterations of scaled-Max-Log-MAP decoding.

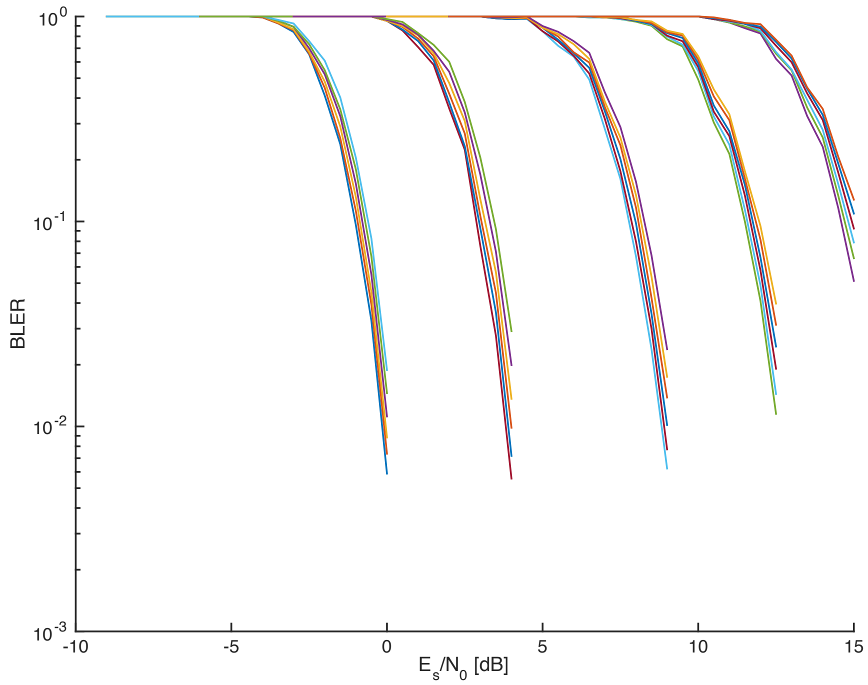

Fig. 14. $K = 80$. $R \in \{1/12, 1/6, 1/3, 1/2, 2/3\}$ from left to right. $L \in \{32, 16, 8, 4, 2, 1\}$ from left to right. 64QAM modulation. AWGN channel. $I = 8$ iterations of scaled-Max-Log-MAP decoding.

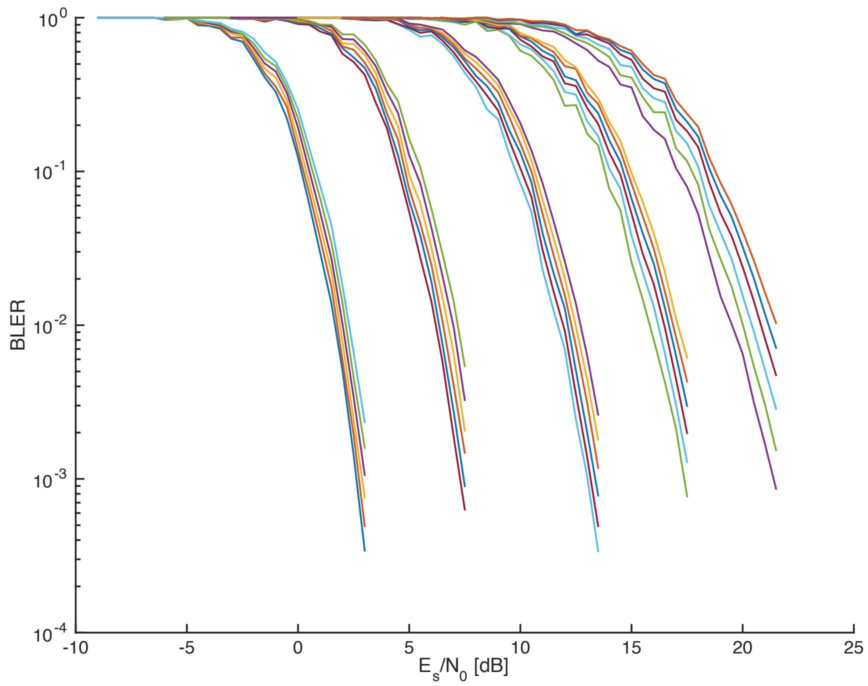

Fig. 15. $K = 32$. $R \in \{1/12, 1/6, 1/3, 1/2, 2/3\}$ from left to right. $L \in \{32, 16, 8, 4, 2, 1\}$ from left to right. 64QAM modulation. Uncorrelated narrowband Rayleigh fading channel. $I = 8$ iterations of scaled-Max-Log-MAP decoding.

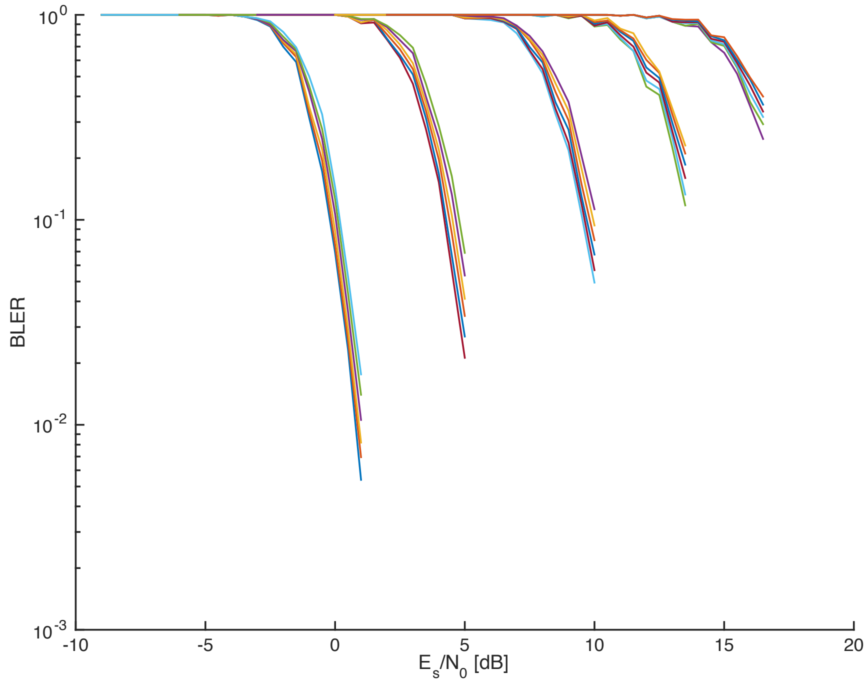

Fig. 16. $K = 80$. $R \in \{1/12, 1/6, 1/3, 1/2, 2/3\}$ from left to right. $L \in \{32, 16, 8, 4, 2, 1\}$ from left to right. 64QAM modulation. Uncorrelated narrowband Rayleigh fading channel. $I = 8$ iterations of scaled-Max-Log-MAP decoding.